2026, Scienceline Publication
World's Veterinary Journal
World Vet J, 16(2): 347-359.
ISSN 2322-4568

DOI: https://dx.doi.org/10.54203/scil.2026.wvj33
PII: S232245682600033-16

Histopathological Insights into Purkinje Cell Responses of Maternal and Fetal Cerebellum in Mice: Electromagnetic Wave Exposure and Protective Role of Cactus (*Opuntia* spp.)

Desy Armalina[1]*, Neni Susilaningsih[1], Heri Sutanto[2] and Sunarno[3]

[1]*Anatomy-Histology Department, Faculty of Medicine, Diponegoro University, Semarang, Indonesia*
[2]*Department of Physics, Faculty of Sciences and Mathematics, Diponegoro University, Semarang, Indonesia*
[3]*Department of Biology, Faculty of Sciences and Mathematics, Diponegoro University, Semarang, Indonesia*

*Corresponding author's Email: desyarmalina@lecturer.undip.ac.id

ORIGINAL ARTICLE
Received: March 15, 2026
Revised: April 19, 2026
Accepted: May 21, 2026
Published: June 25, 2026

ABSTRACT

The rapid expansion of wireless technologies has significantly increased human exposure to electromagnetic fields (EMFs), raising concerns about potential effects on reproductive and developmental health. *Opuntia cochenillifera* (*O. cochenillifera*), a cactus rich in mucilage and mineral oxides, has potential as a bio-based material for reducing the intensity of electromagnetic waves (EMWs) through dielectric and magnetic interactions. The present study aimed to evaluate the effects of EMW exposure on Purkinje cell morphology in maternal and fetal cerebellum and to assess the protective potential of distinct *O. cochenillifera* formulations. A total of 42 pregnant BALB/c mice were randomly divided into six groups, including healthy mice as the positive control group, EMW-exposed mice as the negative control group, and four treatment groups. The treatment groups were subjected to EMW exposure alongside the administration of either fresh cactus, dried cactus gel, or powdered cactus (3 g each). The EMW exposure was administered at a specific absorption rate of 1.74 W/kg throughout gestation. Cerebellar tissues were collected on day 20 for histological analysis and characterized by X-ray fluorescence and Fourier-transform infrared spectroscopy. Histological findings demonstrated that EMW exposure disrupted Purkinje cell alignment and decreased Purkinje cell counts in the negative control group. In contrast, all treatment groups demonstrated preserved cellular structure and morphology comparable to that of the healthy mice. Quantitative analysis confirmed significantly higher cell counts in treated groups than in the negative control group. The current findings indicated that EMW exposure adversely affected cerebellar development, while *O. cochenillifera* exhibited protective effects, supporting its potential as a natural EMF-attenuating material.

Keywords: Cactus, Cerebellum, Electromagnetic wave, Histopathology, Purkinje cell

INTRODUCTION

In recent years, exposure to electromagnetic fields (EMF) has increased significantly due to the widespread use of technological devices and telecommunications networks (Ikinci et al., 2019). While mobile phones, Wi-Fi routers, and wireless systems have improved connectivity, the increasing use of these technologies has raised concerns about their potential biological effects. Previous studies have reported oxidative stress, DNA damage, and other harmful biological responses following EMF exposure in experimental models (Jagetia, 2022; Panagopoulos et al., 2025). However, multiple systematic reviews of human and epidemiological data found limited or inconsistent evidence for adverse physiological effects from Wi-Fi or mobile-phone exposure (Bodewein et al., 2022; Dongus et al., 2022). Regarding reproductive health, considerable uncertainty exists. Despite some studies suggesting that EMF exposure could lead to adverse outcomes such as preterm birth, fetal demise, low birth weight, and congenital anomalies, the epidemiological results are not consistent (Kim et al., 2021). Therefore, the World Health Organization (WHO) International EMF Project has designated reproductive outcomes, oxidative stress, cognitive impairment, and cancer risk as priority areas for investigation (Verbeek et al., 2021). Regulatory authorities, such as the International Commission on Non-Ionizing Radiation Protection (ICNIRP, 2020) and the U.S. Federal Communications Commission (FCC, 2025), have established safety guidelines for mobile devices; however, not all devices consistently adhere to these guidelines. Furthermore, the WHO has identified electromagnetic radiation as one of the most rapidly expanding environmental threats worldwide (Davies et al., 1995).

Microwave radiation, a subset of EMF with frequencies ranging from 300 MHz to 300 GHz, is widely employed in telecommunications, industry, and healthcare (Lahiri, 2023). Numerous studies have documented adverse biological effects of microwave radiation, including structural and functional alterations in the nervous, cardiovascular, reproductive, and endocrine systems (Pall, 2016). In experimental models, pregnant mice exposed to 2.45 GHz electromagnetic waves (EMW) exhibited oxidative stress and morphological disruptions at the placenta-embryo implantation site, resulting in embryo resorption (Shahin et al., 2013). Additionally, epidemiological findings indicated

To cite this paper: Armalina D, Susilaningsih N, Sutanto H, and Sunarno (2026). Histopathological Insights into Purkinje Cell Responses of Maternal and Fetal Cerebellum in Mice: Electromagnetic Wave Exposure and Protective Role of Cactus (*Opuntia* spp.). *World Vet. J.*, 16(2): 347-359. DOI: https://dx.doi.org/10.54203/scil.2026.wvj33

potential associations between prolonged maternal EMF exposure and outcomes like miscarriage, preterm labor, reduced fetal growth, and congenital malformations (Abdul-Al et al., 2022). More evidence indicates that EMF affects overall physiology and brain development (Bodin et al., 2025). Animal studies have demonstrated that extended EMF exposure leads to cortical thinning, neuron loss, and alterations in brain structure (Akakin et al., 2021; Arslan et al., 2022; Eskandani and Zibaii, 2024). At the molecular level, EMF is linked to oxidative stress, mitochondrial dysfunction, and disrupted calcium signaling, all of which compromise neuronal health (Saliev et al., 2019; Lai, 2021; Leach et al., 2025). These disturbances particularly affect the cerebellum, which is crucial for motor coordination and cognitive functions (Cordelli et al., 2023; Mehmet et al., 2024). Previous studies demonstrated that exposure to 900 MHz EMF leads to Purkinje cell degeneration and oxidative imbalance, although antioxidant treatments such as luteolin can mitigate these effects (Arslan et al., 2022). Additionally, a neurobehavioral investigation reported that EMF exposure led to impaired balance and coordination, which may be partially explained by damage to cerebellar neurons (Ganjalikhan-hakemi et al., 2023).

The challenges associated with electromagnetic radiation have prompted the development of materials designed to absorb or block such radiation (Rong et al., 2025). Traditional absorbers, such as conductive materials, dielectric ceramics, and magnetic composites, often encounter challenges including impedance mismatch, high density, and limited biocompatibility (Ren et al., 2025). Consequently, natural plant-based biomaterials have garnered interest due to sustainability, cost-effectiveness, and multifunctional properties (Shi et al., 2025). Agricultural by-products, including porous carbon from coconut shells, *Agave atrovirens*, and *Opuntia ficus-indica* powders, have demonstrated considerable potential for microwave absorption (Simón et al., 2019; Kumar and Kuanr, 2024). Specifically, measurements of reflection, transmission, and absorption parameters between 1.7-2.6 GHz indicated that *Opuntia ficus-indica* acts as a high-loss dielectric material. The presence of a fibrous multilayered internal structure and high-water content promotes greater absorption and lower transmission (Lee et al., 2024; Alves et al., 2025), whereas the observed increase in reflection of the Opuntia material suggests a relatively high dielectric constant. These combined properties support that *Opuntia* can function effectively as a natural electromagnetic shielding material (Erdem, 2026). Based on waveguide measurements, *Opuntia ficus-indica* functioned as a moderate microwave-absorbing material, showing an absorption coefficient near 0.23 in the 8-13 GHz range, which indicated potential applicability of *Opuntia ficus-indica* as a natural electromagnetic shielding material (Simón et al., 2019).

The mechanisms by which Opuntia interacts with EMF, particularly the susceptibility of the fetal cerebellum, remain poorly understood. Therefore, the present study aimed to evaluate the effects of fresh, dried, gel, and powder forms of *Opuntia cochenillifera* (*O. cochenillifera*) as natural dielectric materials in reducing EMFs in pregnant mice, utilizing morphological and spectroscopic analyses to elucidate their interactions with EMW and assess their potential as environmentally friendly shielding materials.

MATERIALS AND METHODS

Ethical approval

Ethical approval for all animal procedures was obtained from the Medical and Health Research Ethics Commission of Diponegoro University, Indonesia (No. 116/EC-H/KEPK/FK-UNDIP/IX/2023). Experiments were conducted in accordance with the institution's guidelines and internationally recognized standards for the care and use of laboratory animals, and reporting follows the ARRIVE recommendations where applicable. Throughout the study, animal welfare was prioritized by minimizing pain, stress, and discomfort. All procedures were carried out by trained personnel to ensure proper handling and reduce distress. Human endpoints and strategies to minimize distress were applied throughout. In addition, the study adhered to the principles of the 3Rs (Replacement, Reduction, and Refinement), and the minimum number of animals necessary to achieve the scientific objectives was used.

Animals

A total of 56 BALB/c mice were used in the present study, consisting of 42 females and 14 males, all aged 2-3 months and weighing 25-30 g. The mice were acclimated to the laboratory environment for seven days, with environmental conditions maintained at 24 ± 2°C, 50-60% humidity, and a 12-hour light/dark cycle. Animals had free access to water and food pellets. Following acclimatization, mating was conducted overnight (12 hours) starting at 6:00 PM, with females and males housed together at a 3:1 female-to-male ratio. The next morning, vaginal plugs and swabs were inspected to confirm mating. Males were immediately removed after confirmation, and only the pregnant females were retained for the study. The pregnant females were then randomly assigned to six experimental groups, with seven mice in each group. The treatment groups consisted of healthy mice serving as the positive control, mice exposed to EMW as the negative control, and four EMW-exposed groups fitted with belts containing fresh, dried gel, or powdered cactus, respectively. Successful breeding was confirmed at gestational days 10 (G10) and 13 (G13), evidenced by a 3-4 g

increase in female body weight. Weight changes were used to monitor pregnancy status, with weight gain indicating successful gestation and sudden loss suggesting prenatal complications or miscarriage (Neres et al., 2008). The pregnant mice were housed in 45 × 45 × 25 cm polypropylene cages, with absorbent wood chip bedding replaced three times daily to maintain clean and comfortable living conditions. Cage positions were rotated regularly to minimize environmental variation.

Experimental design and treatment procedures

The study comprised one healthy control group (HCG) containing mice that were not exposed to EMW radiation, a negative control group (NCG), and four experimental groups (E1-E4). The NCG was exposed to EMW without any protective intervention, whereas the experimental groups (E1-E4) were each fitted with abdominal belts containing different forms of *O. cochenillifera* to mitigate the effects of EMW. Mice in the first experimental group received a belt with fresh cactus sliced into small fragments (E1), mice in the second experimental group received a belt containing sun-dried cactus processed into a coarse powder (E2), in the third experimental group, mice received a belt containing a cactus gel extract prepared by macerating cactus in 70% ethanol and formulated into a gel (E3), and mice in the fourth experimental group received a belt containing cactus powder obtained by dehydrating the gel extract used in E3 into a fine powder (F4). All treatment groups were exposed to continuous EMW radiation from a cellular phone operating at 900 MHz and 2.45 GHz Wi-Fi, with a whole-body specific absorption rate (SAR) of 1.74 W/kg, for 24 hours daily during gestational days 1–19. Each belt was constructed from a sterilized plastic bag filled with one of the cactus preparations (fresh, dried, gel, or powdered extract) and shaped to fit the abdominal contour of the mice. Before application, the abdominal fur was removed to ensure direct skin-to-skin contact. The belt was securely attached using a waterproof adhesive plaster, ensuring uniform positioning and uninterrupted skin contact throughout EMW exposure. The belts were examined daily and replaced as needed to ensure proper hygiene and secure connections.

Belt composition and application

Each therapeutic belt comprised a waterproof adhesive patch measuring 15 × 3 cm, including a 2 × 1 cm central capsule constructed from a modified paper clip. The belt contained the cactus formulation corresponding to each treatment group. The cactus formulations were not administered trans-dermally or orally, and there was no direct biochemical contact with the cutaneous cells or systemic antioxidant mechanisms. The cactus served as a physical interface engineered to reflect or absorb incoming EMWs, providing a non-invasive protective mechanism.

Sample collection

On gestational day 20, euthanasia was performed via intraperitoneal injection of ketamine. Euthanasia was performed via intraperitoneal injection of ketamine (Ket-A-100, injection 100 mg/mL, Indonesia) at a dose of 120 mg/kg body weight, which is commonly used in rodents to induce deep anesthesia and achieve humane euthanasia. The selected dose is within the established range of 85-200 mg/kg for ketamine in mice. Mice were observed for loss of pedal reflex to confirm adequate anesthesia before dissection (Jamal et al., 2008; Hohlbaum et al., 2018). Following confirmation of death, the pregnancy was terminated, and the maternal and fetal cerebellar tissues were carefully dissected. The samples were immediately fixed in 10% neutral buffered formalin for 24-48 hours. After fixation, tissues underwent established paraffin-processing, including graded ethanol dehydration (70%, 80%, 90%, 95%, 100%), xylene clearing, and embedding in paraffin blocks. Paraffin blocks were sectioned at a thickness of 4-5 µm using a rotary microtome and mounted on glass slides. The slides were then subjected to Hematoxylin-Eosin (H&E) staining, consisting of hematoxylin nuclear staining, differentiation, bluing, eosin counterstaining, dehydration, clearing, and coverslip mounting. Histological preparations were examined under a light microscope for structural assessment in accordance with histopathology protocols (Ghoneim and Arafat, 2016; Javaeed et al., 2021).

X-ray Fluorescence analysis

The elemental composition of the *O. cochenillifera* preparations was determined using an energy-dispersive X-ray fluorescence spectrometer (EDX-7000, Shimadzu Corporation, Japan). Samples weighing 0.5-1 g were dried to constant weight, homogenized, and pressed into pellets before analysis. Measurements were carried out at 50 kV and 1 mA with a 200-second acquisition time, and the spectra were analyzed using the manufacturer's energy-dispersive X-ray fluorescence (EDXRF) software package (Santo et al., 2025).

Fourier transform infrared spectroscopy analysis

Functional group characterization was performed using a Fourier transform infrared spectrometer equipped with a diamond attenuated total reflectance (ATR) accessory (IRSpirit ATR, Shimadzu Corporation, Japan). Spectra were collected from 4000-400 cm^{-1} with a resolution of 4 cm^{-1} and 32 scans per sample. Baseline correction and normalization were performed using the built-in LabSolutions IR software (Gieroba et al., 2023).

Statistical analysis

All statistical analyses were performed using SPSS version 26.0. Data normality was assessed using the Shapiro-Wilk test, which indicated a non-normal distribution for cerebellar tissue examinations in both maternal and fetal samples. Therefore, nonparametric statistical methods were employed for group comparisons. The Kruskal-Wallis test was used to compare across groups, followed by post-hoc pairwise comparisons using the Mann-Whitney U test. The present results were presented as mean ± standard deviation (SD), with statistical significance defined as a p-value less than 5% ($p < 0.05$).

RESULTS AND DISCUSSION

The HCG exhibited Purkinje cells arranged in a continuous monolayer at the junction of the molecular and granular layers, characterized by large euchromatic nuclei and intact morphology. In contrast, the NCG revealed disorganized Purkinje cell alignment, reduced cellularity, and degenerative features, including pyknotic nuclei and areas of focal loss.

In the treatment groups (E1-E4), Purkinje cells remained detectable as a distinct monolayer, with only minimal degenerative changes compared to the NCG. Group E1 exhibited a well-preserved morphology, closely resembling HCG. Groups E2-E4 demonstrated a well-defined Purkinje cell layer characterized by decreased yet recognizable cellular alignment, and overall histological preservation was greater than that observed in the NCG.

The descriptive results indicated that the HCG and treatment groups (E1-E4) exhibited relatively comparable Purkinje cell size and count, with mean values ranging from 1.39-1.40 µm for cell size and 9.4-9.6 cells for cell count. In contrast, the NCG consistently demonstrated reduced values, with an average Purkinje cell size of 1.13 ± 0.22 µm and a cell count of 4.80 ± 2.00. A similar trend was observed in fetal Purkinje cell measurements, with NCG values remaining significantly lower than those in the HCG and E1–E4 groups (Table 1). Significant overall differences were observed across all six groups (HCG, NCG, E1, E2, E3, and E4) for Purkinje cell size and count, as well as for fetal parameters ($p < 0.05$). The NCG demonstrated statistically significant differences compared to the HCG and all treatment groups for all parameters ($p < 0.05$). However, no statistically significant differences were found among the experimental groups (E1-E4), nor between the HCG and any of the experimental groups ($p > 0.05$). The current findings suggested that the experimental interventions effectively maintained Purkinje cell morphology at levels comparable to HCG, whereas NCG consistently exhibited impairment across all parameters.

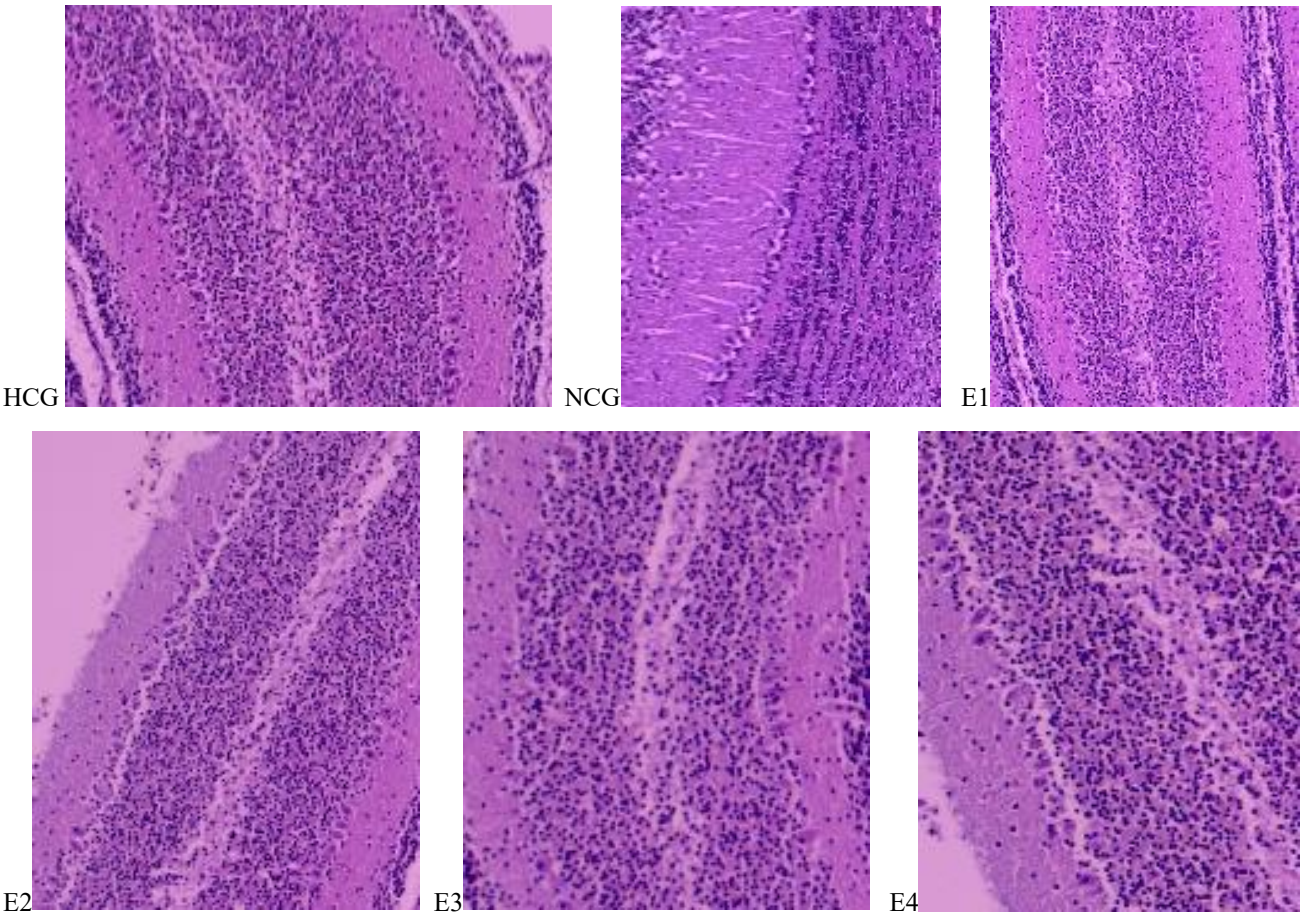

Figure 1. Mice fetal cerebellar Purkinje cell. HCG: Health control group, NGC: Negative control group, E1: Fresh cactus belt (raw cactus), E2: Desiccated cactus belt, E3: Cactus extract gel belt, E4: Cactus extract powder belt (dehydrated extract). H&E, 400×.

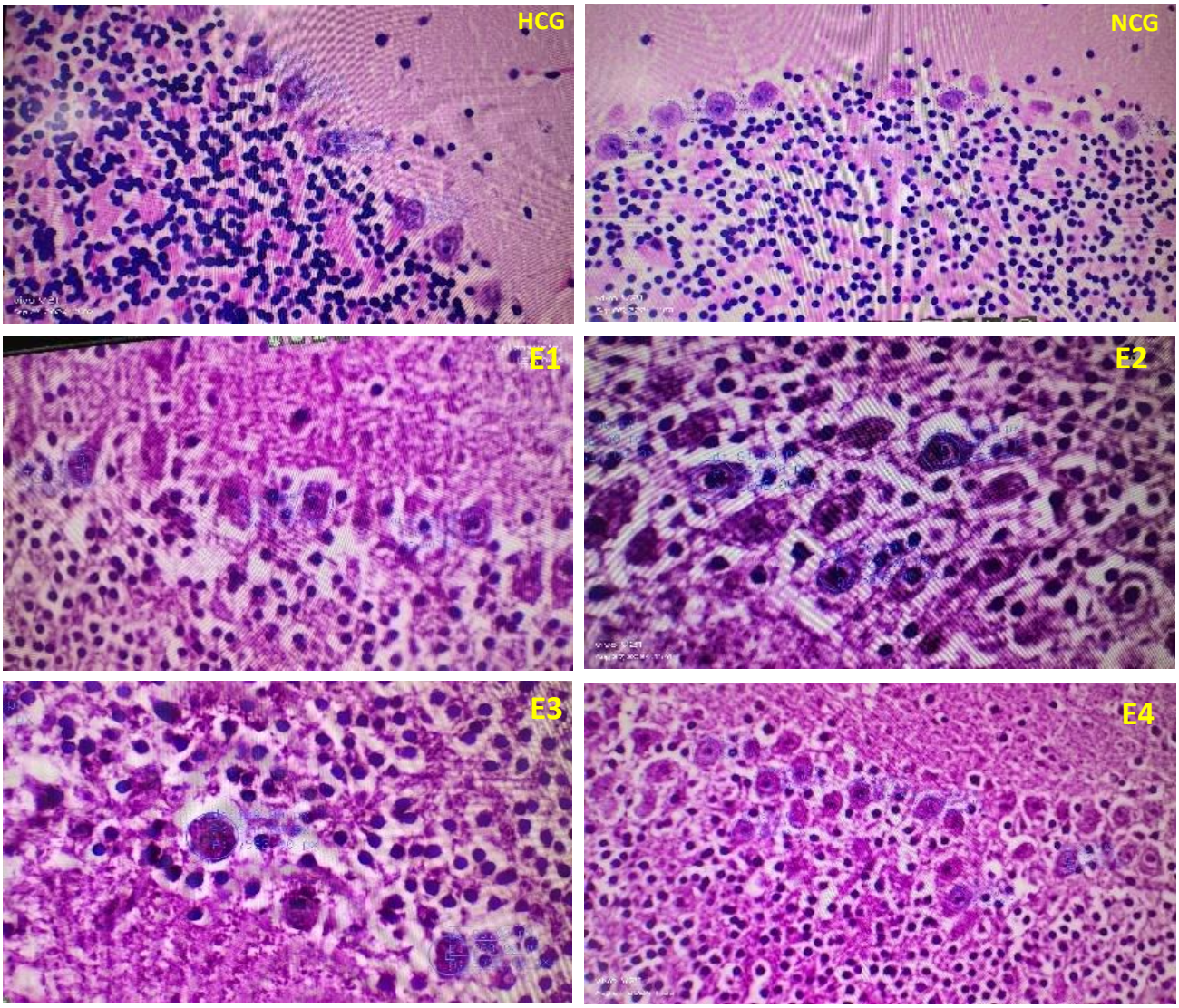

Figure 2. Maternal cerebellar Purkinje cells of Female 2-3 months old mice. HCG: Health control group, NGC: Negative control group, black arrow: Reduced number of cells, E1: Fresh cactus belt (raw cactus), E2: Desiccated cactus belt, E3: Cactus extract gel belt, E4: Cactus extract powder belt (dehydrated extract). H&E, ×400.

Table 1. Effects of cactus-based interventions on maternal and fetal Purkinje cell size and count across experimental groups

Group	Maternal Purkinje Size (µm)	Maternal Purkinje Count	Fetal Purkinje Size (µm)	Fetal Purkinje Count	P value
HCG	1.39 ± 0.20[a]	9.60 ± 1.80[a]	1.37 ± 0.22[a]	9.40 ± 2.10[a]	<0.000
NCG	1.13 ± 0.22[b]	4.80 ± 2.00[b]	1.09 ± 0.19[b]	4.60 ± 1.80[b]	-
E1	1.40 ± 0.23[a]	9.50 ± 1.70[a]	1.38 ± 0.24[a]	9.50 ± 1.90[a]	<0.000
E2	1.40 ± 0.21[a]	9.40 ± 1.80[a]	1.39 ± 0.23[a]	9.60 ± 1.70[a]	<0.000
E3	1.39 ± 0.22[a]	9.60 ± 1.90[a]	1.37 ± 0.20[a]	9.50 ± 2.00[a]	<0.000
E4	1.39 ± 0.19[a]	9.50 ± 1.80[a]	1.38 ± 0.21[a]	9.40 ± 1.80[a]	<0.000

HCG: Healthy control group, NCG: Negative control group, E1: Fresh cactus belt (raw cactus), E2: Desiccated cactus Belt, E3: Cactus extract gel belt, E4: Cactus extract powder belt. P values were calculated relative to the negative control group (NCG). Data are expressed as mean ± standard deviation (SD). [ab]Means significant differences between groups are indicated by different superscript letters within the same column, as determined by Mann–Whitney post hoc tests following Kruskal–Wallis analysis ($p < 0.05$).

Mineral composition and Fourier transform infrared spectroscopy

The results of the X-ray fluorescence demonstrated notable differences in mineral compositions among the raw cactus, dried cactus, cactus extract gel, and cactus extract powder preparations (Table 2). Dried cactus demonstrated the highest calcium oxide (CaO) concentration of 1.90%, whereas the cactus extract gel was significantly enriched in

potassium oxide (K_2O, 8.45%) and chloride (Cl, 5.43%). Magnesium oxide (MgO) was significantly elevated in the cactus extract gel (1.49%) compared to the other forms of cactus. Trace elements such as iron (III) oxide (Fe_2O_3), silver oxide (Ag_2O), and iodine were mostly identified in the raw cactus, whereas bromine (Br) was exclusively present in the cactus extract gel and powder.

Fourier-transform infrared (FTIR) spectroscopy revealed essential functional groups in all samples (Table 3). Raw cactus spectra revealed significant hydroxyl stretching (3305 cm^{-1}), carbonyl amide (1636 cm^{-1}), and ether/polysaccharide peaks, indicative of elevated water and carbohydrate contents. Dried cactus exhibited preserved hydroxyl and aromatic ring signals and heightened ester/protein-associated peaks. The cactus extract gel demonstrated pronounced carbonyl stretching (1722 cm^{-1}), suggestive of esters or carboxylic acids, and aromatic and amine functionalities. The cactus extract powder exhibited pronounced hydroxyl and phenolic signals, intricate polysaccharide bands, and substituted aromatic ring patterns. The current results indicated that drying increased the CaO and K_2O. Simultaneously, extraction, especially in the gel form, significantly enriched K_2O, Cl, and MgO, along with notable functional groups associated with aromatic compounds and polysaccharides. The variability in biological activities among the cactus forms might be attributed to the differences in their chemical and structural characteristics.

Table 2. Mineral contents of cactus preparations determined by X-ray fluorescence

Mineral	Raw cactus	Dried cactus	Cactus extract gel	Cactus extract powder
CaO	0.288%	1.90%	0.05%	0.12%
MgO	0.0728%	0.353%	1.49%	0.0953%
K_2O	0.0553%	1.37%	8.45%	0.764%
Cl	0.0683%	0.245%	5.43%	0.349%
Trace elements	Fe_2O_3, Ag_2O, I, RuO_2, TeO_2, ZrO_2/Nb_2O_5	Fe_2O_3, P_2O_5, SO_3, SrO	Br, P_2O_5, SO_3, Rb_2O	P_2O_5, SO_3, Br, Rb_2O

CaO: Calcium oxide, MgO: Magnesium oxide, K_2O: Potassium oxide, Cl: Chloride, Fe_2O_3: Iron (III) oxide, Ag_2O: Silver oxide, I: Iodine, RuO_2: Ruthenium oxide, TeO_2: Tellurium oxide, ZrO_2: Zirconium oxide, Nb_2O_5: Niobium oxide, P_2O_5: Phosphorus pentoxide, SO_3: Sulfur trioxide, SrO: Strontium oxide, Br: Bromine, Rb_2O: Rubidium oxide

Table 3. Representative Fourier transform infrared spectroscopy bands and assigned functional groups observed across cactus-derived samples

Sample	Main peaks (cm^{-1})	Key functional group
Raw cactus	3305 (O–H), 2110 (Alkyne/N=C=O), 1636 (C=O amide), 1018 (C–O–C)	Hydroxyl, amide, ether/polysaccharide, reactive triple bond
Dried cactus	3265 and 2917 (O–H, C–H), 1606 (C=C aromatic), 1316 and 1033 (C–O/C–N ester)	Hydroxyl, aromatic ring, ester/protein
Cactus extract gel	3217 (O–H), 1722 (C=O ester), 1584 (C=C aromatic/N–H), 1047 (C–O)	Hydroxyl, ester/carboxylic acid, aromatic/amine, carbohydrate
Cactus extract powder	3324 (O–H), 1593 (C=C aromatic/amide), 1030–1068 (C–O), 749 and 670 (Aromatic sub.)	Hydroxyl, phenolic, polysaccharide, substituted aromatic rings

Impacts of electromagnetic waves on maternal and fetal Purkinje cells

The present study demonstrated that Purkinje cell size and count in the HCG and experimental groups (E1-E4) were maintained at comparable levels. In contrast, the NCG exhibited significantly reduced values and distinct histological degeneration ($p < 0.05$). The present findings indicated that exposure to EMFs without protective measures compromised cerebellar integrity, whereas controlled interventions were able to mitigate this damage.

Purkinje cells, which serve as the primary neurons of the cerebellar cortex, exhibited high susceptibility to oxidative stress because of elevated metabolic demands, complex dendritic architecture, and mitochondrial dependence (Altunkaynak et al., 2016; Manolaras et al., 2023; Chui et al., 2024). Increased reactive oxygen species (ROS) can lead to mitochondrial malfunction, lipid peroxidation, protein oxidation, and DNA damage, ultimately inducing apoptosis through caspase activation and jeopardizing neuronal survival (Chen et al., 2003; Liu et al., 2025; Toader and Covache-busuioc, 2025). The impairment of ion channel function and synaptic communication has been implicated as a contributing factor, further disrupting Purkinje cell physiology and heightening the risk of degeneration (Orfali et al., 2024). Furthermore, oxidative stress can compromise ion channel function by inducing oxidative modifications in protein channels, which alter the gating properties of voltage-gated and ligand-gated ion channels, further disrupting neuronal physiology and enhancing vulnerability to degeneration (Georgiou and Margaritis, 2021; Orfali et al., 2024).

Previous studies examining the effects of 900-MHz EMFs on the cerebellum using histopathological and immunohistochemical techniques reported the presence of pyknotic nuclei in Purkinje cells and granular layer neurons, along with a marked reduction in cytoplasmic content in the EMF-exposed groups (Bas et al., 2022). Depending on the frequency, intensity, and duration of exposure, EMWs can produce diverse cellular effects. Ion channel impairment occurs through a mechanism in which non-ionizing EMFs disturb the electrochemical balance across cellular membranes, modify cation flux, and impair voltage-gated ion channel function. Such disturbances may increase oxidative stress through the activation of membrane-associated enzymes such as NADPH oxidase (NOX), resulting in the overproduction of ROS, compromised cellular function, and even DNA damage, which is implicated in carcinogenesis (Georgiou and Margaritis, 2021; Panagopoulos and Karabarbounis, 2021). Several studies have indicated that EMF-induced disruption of ion channels was associated with the generation of ROS and oxidative stress via NOX activation, resulting in subsequent cellular damage, including DNA strand breaks (Georgiou and Margaritis, 2021). The specific function of NOX in facilitating oxidative stress during EMF exposure continues to be a primary focus of investigations (Georgiou and Margaritis, 2021).

Cellular stress response

Exposure to non-ionizing EMF activates a cellular stress response, a protective mechanism designed to preserve cellular integrity (Lai and Levitt, 2024). The cellular response involves a series of molecular and cellular alterations, such as cell cycle arrest and activation of repair mechanisms to manage macromolecular damage (Meyer et al., 2024). This cellular reaction is not specific to EMF but is a general reaction to several stressors and can lead to repair or, in cases of severe damage, cell death (Haidar et al., 2025). The stress response follows a non-linear pattern dependent on dose and timing and may influence several health outcomes, such as cancer risk and nerve regeneration (Lai and Levitt, 2024). These approaches revealed the complex nature of EMWs' interactions with biological systems (Meyer et al., 2024). Biological responses to EMF were substantially affected by the parameters of exposure. While excessive or improperly regulated exposure may lead to oxidative stress and cellular damage, carefully controlled EMF application has been associated with adaptive or therapeutic effects, such as enhanced tissue repair and increased bacterial susceptibility to antibiotics (Haidar et al., 2025).

The cerebellar alterations observed in the present study are consistent with the cellular stress response described in the literature. Exposure to non-ionizing EMFs triggered a conserved cellular defense response characterized by cell-cycle arrest, enhanced DNA and protein repair pathways, and, in instances where damage surpassed repair capacity, apoptotic cell death (Lai and Levitt, 2024). The observed mechanistic pattern aligned with the structural disruptions noted in maternal and fetal cerebella following EMF exposure, suggesting that cerebellar tissue experienced a transition toward maladaptive stress responses.

Oxidative stress has been widely identified as a central mediator of EMF-induced cellular injury in neural tissues. Numerous *in vitro* and *in vivo* studies have demonstrated that EMF exposure increased ROS, disrupted mitochondrial function, and promoted oxidative DNA and protein damage (Saliev et al., 2019; Schuermann and Mevissen, 2021). The findings of reduced Purkinje cell counts and altered cerebellar morphology in fetal mice, alongside corresponding changes in EMF-exposed dams, were related to these mechanisms. The cerebellum, particularly Purkinje neurons, is highly susceptible to oxidative imbalance, which aligns with the ROS-driven injury observed in the present study (Schuermann and Mevissen, 2021).

According to multiple studies, EMF biological effects are strongly influenced by exposure dose, duration, developmental stage, and the inherent vulnerability of neural tissue (Tian et al., 2022; Lai and Levitt, 2024). These findings are consistent with the more pronounced alterations observed in fetal cerebellar tissue in the present study, as the developing brain exhibits immature antioxidant defenses and a higher proliferative index, making it especially vulnerable to EMF-induced oxidative stress and stress-response activation. Consequently, although EMF exposure may result in adaptive or neutral outcomes, the prenatal cerebellum is far more likely to experience growth impairment or structural disruption under the same exposure conditions (Tian et al., 2022).

Potential electromagnetic wave attenuation and mineral composition

Iron oxide (Fe_2O_3) is widely known as an effective microwave absorber owing to its dual contribution to magnetic and dielectric loss mechanisms (Akinay et al., 2023; Ghosh et al., 2023). Incorporating α-Fe_2O_3 nanostructures into composites has indicated delivering reflection loss values greater than −30 dB within the gigahertz range, largely due to interfacial polarization and magnetic resonance effects (Mensah et al. 2022; Zheng et al., 2022). The notable EMW absorption capacity of Fe_2O_3-based materials in engineered composites, attributed to combined magnetic and dielectric loss, suggested that even low concentrations of Fe_2O_3 particles within biological matrices may contribute to partial wave attenuation before deep tissue penetration (Lesbayev et al., 2025; Lodi et al., 2025).

In contrast, CaO and MgO function predominantly as dielectric agents, enhancing polarization under alternating EMFs. The MgO-based ceramics and glass-ceramics are widely used for dielectric applications in microwave and radiofrequency systems (Hu et al., 2021). The current results demonstrated that MgO or CaO/MgO mixtures could serve as dielectric buffers in composite matrices (Cabeza et al., 2002). The ability of such oxide particles to attenuate incident EMFs when incorporated into biological tissues has not yet been experimentally validated, necessitating focus on *in vivo* investigations (Lodi et al., 2025; Reghunath et al., 2025a). The observed polarization causes dipole alignment and energy loss, converting electromagnetic energy into localized heat at the microstructural level (Muradyan et al., 2025). Under these conditions, dried cactus preparations demonstrated the highest combined CaO and MgO content, suggesting a strong dielectric contribution to EMW attenuation.

Potassium oxide (K_2O), which was relatively abundant in the cactus gel, may help modulate the local dielectric properties of the hydrated matrix. Absorption efficiency in engineered EMW-absorbing materials relies heavily on precise control of permittivity and impedance matching with free space, typically achieved through dielectric and/or magnetic loss mechanisms (Gabriel et al., 1996a; Ruscica et al., 2024). Any involvement of K_2O-rich biological matrices in modulating impedance and attenuating EMW remains theoretical, as no direct *in vivo* data are currently available (Akinay et al., 2023; Chen et al., 2024). The combination of K_2O-rich domains and organic components facilitates dielectric heterogeneity, resulting in enhanced multiple scattering and efficient attenuation of EMW transmission (Reghunath et al., 2025b).

The presence of chloride ions (Cl^-) in hydrated matrices can influence ionic conductivity, dielectric response, and microstructural organization, thereby modulating the interaction of these materials with alternating EMFs. Studies have documented this effect in inorganic composites like chloride-exposed cement pastes, where Cl^- alters impedance and dielectric behavior. However, whether similar effects happen in biological gcenchenels remains unknown and has not been proven (Hu et al., 2016).

Chloride ions increase ionic conductivity in hydrogels, a useful property for sensors (Ji et al., 2025). In cement materials, chloride and moisture changes can alter electrical properties and create irregularities that scatter, reflect, or reduce EMWs (Hu et al., 2019, 2020; Elseady et al., 2023; Mizobuchi et al., 2026). Cl^- affects ion distribution and interfacial conductivity in anti-corrosion coatings, thereby altering wave propagation through the material (Zhang et al., 2021; Tzaneva and Kostov, 2023). These mineral oxides and salts contribute to three principal electromagnetic attenuation mechanisms. Iron oxide (Fe_2O_3) predominantly promoted magnetic loss through the hysteresis mechanism and eddy-current dissipation, while dielectric oxides such as CaO, MgO, and K_2O enhanced dielectric loss via dipole polarization and relaxation under alternating EMFs (Zhang et al., 2022; 2025). Additionally, components such as K_2O and Cl^- can induce impedance mismatch and microstructural heterogeneity in hydrated matrices, leading to multiple scattering and reflection that further reduce EMW transmission (Liang et al., 2021; Katheriya et al., 2025).

Interaction of dielectrics with organic functional groups

The FTIR spectroscopy analysis provided insight by identifying organic functional groups capable of interacting with EMW. All cactus samples displayed pronounced O–H stretching bands between 3200 and 3500 cm^{-1}, indicating the existence of hydroxyl-rich compounds, such as phenolics and polysaccharides. These functional groups demonstrated high polarity, allowing interaction with alternating electric fields in the gigahertz range via mechanisms such as dipole rotation and dielectric heating, as reported by Gabriel et al. (1996b), Soria et al. (2021), and Wang et al. (2023).

Cactus gel and powder extracts exhibited significant C=O stretching bands at approximately 1720 cm^{-1}, indicative of esters and carboxylic acids. Carboxyl groups improved hydrophilicity and surface polarity, yet recent findings indicated that their effectiveness in reducing EMWs may rely on their interactions with conductive elements. In hydrated matrices, these groups may still promote the dissipation of microwave energy via intermolecular collisions (Płowaś-Korus and Buchner, 2021). The C-O stretching region (1030-1068 cm^{-1}) observed in all samples indicated the presence of polysaccharides capable of forming hydrogen-bonded networks. These networks, especially when ionically crosslinked with Ca^{2+} or Mg^{2+} derived from the mineral component, can create inhomogeneous dielectric domains within the polymer matrix. These domains enhanced electromagnetic dispersion and reduced the penetration depth in bio-based composites (Prashanth et al., 2024). The aromatic C=C vibrations detected in the dried cactus and gel extract during the present study indicated the presence of phenolic compounds that may participate in π-electron resonance interactions with EMEs. These interactions may contribute slightly to overall EMEs reduction, despite being less efficient than ionic or polar processes.

Coordinated neuroprotective effects on the maternal and fetal cerebellum

The preservation of cerebellar profiles in the cactus-treated groups was likely attributable to the synergistic action of mineral- and organic-based attenuation mechanisms. Mineral oxides act as inorganic shielding agents, contributing to

stable dielectric and magnetic losses, whereas organic polar groups enable dynamic dipole-based dissipation. This dual-mode attenuation reduces the net EMW energy reaching the cerebellum, thereby minimizing microstructural disruption. From a biological perspective, reduced EMW exposure may result in preserved Purkinje cell morphology, decreased neuronal apoptosis, and maintained organization of the cerebellar layers. Although inflammatory and oxidative stress biomarkers were not directly measured, histological assessments of the present study supported the neuroprotective effect. Differences among the cactus preparations may stem from their composition. Dried cactus is rich in CaO and MgO, exhibiting strong dielectric loss potential. Cactus gel extract had very high levels of K_2O and Cl, which enhance scattering and impedance mismatch. Cactus powder extract contained a balanced mix of minerals and organic matter, offering stable shielding. Raw cactus had lower oxide levels but higher water content, which might have promoted dielectric heating and scattering through water dipoles. Although substantial differences were observed in the XRF and FTIR profiles among the four *O. cochenillifera* formulations (raw, dried, gel extract, powder), no considerable differences were detected in the cerebellar outcomes of maternal and fetal mice. The current findings indicated that electromagnetic shielding was influenced less by specific mineral levels and more by collective physicochemical features such as bound water content, ionic composition, and polysaccharide matrix structures (Simón et al., 2019). According to foundational studies on dielectric properties, water dipole polarization and ionic conduction are the primary factors influencing the dielectric behavior of biological and hydrated plant materials, whereas differences in mineral composition have only a limited effect on radiofrequency (RF) reduction (Meenu et al., 2025).

Microwave absorption studies on plant-based materials such as *Opuntia* have revealed that cladodes exhibited high absorption coefficients, a characteristic attributed to their hydrated polysaccharide framework, even when chemical composition differs (Gupta et al., 2024). Consequently, all four cactus formulations probably provided sufficient dielectric shielding to prevent RF exposure from reaching biologically damaging levels. The neuroprotective effects were similar across all cactus formulations, despite differences in their XRF/FTIR profiles.

CONCLUSION

All four forms of *O. cochenillifera*, including raw, dried, gel extract, and powder, demonstrated comparable neuroprotective effects. Each cactus preparation, regardless of its differing XRF and FTIR profiles, provided robust dielectric shielding. This protection effectively prevented EMW-induced cerebellar damage and maintained the morphology and number of maternal and fetal Purkinje cells, achieving levels similar to those of healthy mice. The current findings indicated that the observed neuroprotective effects stem from common physicochemical properties shared across the cactus preparations, rather than from any single form. Therefore, cactus-derived materials show potential as effective, bio-based agents for protecting the nervous system from EMW exposure during pregnancy. This approach offered a sustainable and safer alternative to conventional synthetic composites, with particular relevance for maternal health due to the heightened vulnerability of pregnant individuals to EMW exposure. Future studies should focus on long-term neurodevelopmental investigations on maternal and fetal cerebellar structures, mechanistic investigations clarifying oxidative stress and signaling pathways underlying EMW-induced cerebellar alterations, and optimization of cactus extract formulations to maximize neuroprotective efficacy during pregnancy.

DECLARATIONS

Acknowledgments

The authors would like to acknowledge the Laboratory of the Faculty of Medicine, Universitas Diponegoro, Indonesia, for providing laboratory assistance.

Authors' contributions

Desy Armalina was responsible for the conceptualization and design of the study, coordination and administration of the project, preparation of *O. cochenillifera* materials (including fresh, dried, gel, and powdered forms), oversight of animal scheduling and logistical arrangements, supervision of the *in vivo* phase, and served as the corresponding author while also contributing to the writing of the original draft. Heri Sutanto contributed to the methodology for EMW exposure, including the setup and calibration of the EMW system and exposure parameter instrumentation, performed FTIR and XRF characterization of cactus preparations, and was involved in data curation, visualization, as well as writing, reviewing, and editing of the present study. Sunarno conducted animal handling and randomization, executed the exposure sessions, performed dissection and collection of maternal and fetal cerebella, carried out histology processing and Purkinje-cell morphometry, completed fetal anthropometric assessments, and contributed to data curation, formal analysis, and writing, review, and editing of the manuscript. Neni Susilaningsih supervised the histopathological assessments, interpreted cerebellar findings, integrated mechanistic context related to dielectric and magnetic interactions and mineral-oxide content with experimental results, provided analytical guidance, and performed critical revision of the manuscript, wrote, reviewed, and edited the present study. All authors verified the underlying

data, contributed to data interpretation, agreed to be accountable for all aspects of the study, and approved the final edition of the manuscript.

Availability of the data and materials

All data generated or analyzed during the present study are included in the published article. No additional datasets are available.

Competing interests

The authors have not declared any conflict of interest.

Ethical considerations

The authors confirm that this manuscript is original and not derived from previously published works. An artificial intelligence tools (Grammarly) was only used for language improvement.

Funding

The present study received no external funding.

REFERENCES

Abdul-Al M, Amar ASI, Elfergani I, Littlehales R, Parchin NO, Al-Yasir Y, See CH, Zhou D, Abidin ZZ, Alibakhshikenari M et al. (2022). Wireless electromagnetic radiation assessment based on the specific absorption rate (SAR): A review case study. Electronics, 11(4): 511. DOI: https://www.doi.org/10.3390/electronics11040511

Akakin D, Tok OE, Anil D, Akakin A, Sirvanci S, Sener G, and Ercan F (2021). Electromagnetic waves from mobile phones may affect rat brain during development. Turkish Neurosurgery, 31(3): 412-421. DOI: https://www.doi.org/10.5137/1019-5149.jtn.31665-20.2

Akinay Y, Gunes U, and Cetin T (2023). Recent progress of electromagnetic wave absorbers: A systematic review and bibliometric approach. Chemical Physics and Materials, 2(3): 197-206. DOI: https://www.doi.org/10.1016/j.chphma.2022.10.002

Altunkaynak BZ, Altun G, Yahyazadeh A, Kaplan AA, Deniz OG, Türkmen AP, Önger ME, and Kaplan S (2016). Different methods for evaluating the effects of microwave radiation exposure on the nervous system. Journal of Chemical Neuroanatomy, 75(PartB): 62-69. DOI: https://www.doi.org/10.1016/j.jchemneu.2015.11.004

Alves N, Cavalcanti T, Pereira EM, Gomes JP, Pereira W, and Gonçalves C (2025). Exploring cactus mucilage for sustainable food packaging: A bibliometric review of a decade of research. Processes, 13(6): 1830. DOI: https://www.doi.org/10.3390/pr13061830

Arslan A, Acer N, Kesici H, Sonmez MF, Ertekin T, Gultekin M, Dagdelen U, and Saracoglu OG (2022). Stereological study on the effect of carnosine on Purkinje cells in the cerebellum of rats exposed to 900 MHz electromagnetic field. Turkish Neurosurgery, 32(4): 618-624. DOI: https://www.doi.org/10.5137/1019-5149.JTN.35313-21.2

Bas O, Sengul I, Bas OFM, Hanci H, Degermenci M, Sengul D, Altuntas E, Soztanaci US, and Sonmez OF (2022). Impressions of the chronic 900-MHz electromagnetic field in the prenatal period on Purkinje cells in male rat pup cerebella: Is it worth mentioning?. Revista da Associação Médica Brasileira, 68(10): 1383-1388. DOI: https://www.doi.org/10.1590/1806-9282.20220893

Bodewein L, Dechent D, David G, Thomas K, Tobias K, and Driessen S (2022). Systematic review of the physiological and health-related effects of radiofrequency electromagnetic field exposure from wireless communication devices on children and adolescents. PLoS ONE, 17(6): e0268641. DOI: https://www.doi.org/10.1371/journal.pone.0268641

Bodin R, Godin L, Mougin C, Lecomte A, Larrigaldie V, Feat-Vetel J, Méresse S, Montécot-Dubourg C, Marcelo P, Mortaud S et al. (2025). Altered development in rodent brain cells after 900 MHz radiofrequency exposure. NeuroToxicology, 111: 103312. DOI: https://www.doi.org/10.1016/j.neuro.2025.103312

Cabeza M, Merino P, Miranda A, Nóvoa XR, and Sanchez I (2002). Impedance spectroscopy study of hardened Portland cement paste. Cement and Concrete Research, 32(6): 881-891. DOI: https://www.doi.org/10.1016/S0008-8846(02)00720-2

Chen P, Peng C, Luff J, Spring K, Watters D, Bottle S, Furuya S, and Lavin MF (2003). Oxidative stress is responsible for deficient survival and dendritogenesis in Purkinje neurons from Ataxia-Telangiectasia mutated mutant mice. Journal of Neuroscience, 23(36): 11453-11460. Available at: https://www.jneurosci.org/content/23/36/11453

Chen G, Li Z, Zhang L, Chang Q, Chen X, Fan X, Chen Q, and Wu H (2024). Mechanisms, design, and fabrication strategies for emerging electromagnetic wave-absorbing materials. Cell Reports Physical Science, 5: 102097. DOI: https://www.doi.org/10.1016/j.xcrp.2024.102097

Chui T, Leung S, Fields E, Rana N, Yi R, Shen L, Bernstein AE, Cook AA, Phillips DE, and Watt AJ (2024). Mitochondrial damage and impaired mitophagy contribute to disease progression in SCA6. Acta Neuropathologica, 147(1): 26. DOI: https://www.doi.org/10.1007/s00401-023-02680-z

Cordelli E, Ardoino L, Benassi B, Consales C, Eleuteri P, Marino C, Sciortino M, Villani P, Brinkworth MH, Chen G et al. (2023). Effects of radiofrequency electromagnetic field (RF-EMF) exposure on pregnancy and birth outcomes: A systematic review of experimental studies on non-human mammals. Environment International, 180: 108178. DOI: https://www.doi.org/10.1016/j.envint.2023.108178

Davies MG, Fulton GJ, and Hagen PO (1995). Clinical biology of nitric oxide. British Journal of Surgery, 82(12): 1598-1610. DOI: https://www.doi.org/10.1002/bjs.1800821206

Dongus S, Jalilian H, Schürmann D, and Röösli M (2022). Health effects of WiFi radiation: A review based on systematic quality evaluation. Critical Reviews in Environmental Science and Technology, 52(19): 3547-3566. DOI: https://www.doi.org/10.1080/10643389.2021.1951549

Elseady AAE, Lee I, Zhuge Y, Ma X, Chow CWK, and Gorjian N (2023). Piezoresistivity and AC impedance spectroscopy of cement-based sensors: Basic concepts, interpretation, and perspective. Materials, 16(2): 768. DOI: https://www.doi.org/10.3390/ma16020768

Erdem E (2026). Measurement and comparison of electromagnetic shielding efficiency of hybrid knitted fabrics at X-band. Journal of Engineered Fibers and Fabrics, 21: 1-11. DOI: https://www.doi.org/10.1177/15589250261430874

Eskandani R and Zibaii MI (2024). Unveiling the biological effects of radio-frequency and extremely-low frequency electromagnetic fields on central nervous system performance. BioImpacts, 14(4): 30064. DOI: https://www.doi.org/10.34172/bi.2023.30064

Federal communications commission (FCC) (2025). Specific absorption rate (SAR) for cellular telephones. Available at: https://www.fcc.gov/general/specific-absorption-rate-sar-cellular-telephones

Gabriel S, Lau RW, and Gabriel C (1996a). The dielectric properties of biological tissues: III. Parametric models for the dielectric spectrum of tissues. Physics in Medicine & Biology, 41(11): 2271. DOI: https://www.doi.org/10.1088/0031-9155/41/11/003

Gabriel S, Lau RW, and Gabriel C (1996b). The dielectric properties of biological tissues: II. Measurements in the frequency range 10 Hz to 20 GHz. Physics in Medicine and Biology, 41(11): 2251-2269. DOI: https://www.doi.org/10.1088/0031-9155/41/11/002

Ganjalikhan-hakemi S, Gholamreza A, Majid AS, and Masoumeh N (2023). Agmatine improves neuronal damage and oxidative stress in brain tissue. Brain and Behavior, 13(1): e3124. DOI: https://www.doi.org/10.1002/brb3.3124

Georgiou CD and Margaritis LH (2021). Oxidative stress and NADPH oxidase: Connecting electromagnetic fields, cation channels and biological effects. International Journal of Molecular Sciences, 22(18): 10041. DOI: https://www.doi.org/10.3390/ijms221810041

Ghoneim FM and Arafat EA (2016). Histological and histochemical study of the protective role of rosemary extract against harmful effect of cell phone electromagnetic radiation on the parotid glands. Acta Histochemica, 118(5): 478-485. DOI: https://www.doi.org/10.1016/j.acthis.2016.04.010

Ghosh NN, An YJ, Nishida K, Yamamoto T, Ueda S, and Deguchi T (2023). Dielectric microwave absorbing structures. Frontiers in Materials, 10: 1181978. DOI: https://www.doi.org/10.3389/fmats.2023.1181978

Gieroba B, Kalisz G, Krysa M, Khalavka M, and Przekora A (2023). Application of vibrational spectroscopic techniques in the study of natural polysaccharides and their cross-linking process. International Journal of Molecular Sciences, 24(3): 2630. DOI: https://www.doi.org/10.3390/ijms24032630

Gupta H, Rai MK, and Khanna R (2024). Performance evaluation of microwave absorbers based on biodegradable agricultural waste materials in the X-band. Proceedings of IEEE Conference, 19: 1-6. DOI: https://www.doi.org/10.1109/i2ct61223.2024.10543603

Haidar J, Nabos P, Orlacchio R, Hurtier A, De Gannes FP, Rambert J, Cario-André M, Moisan F, Rezvani H, Lagroye I et al. (2025). Impact of *in vitro* exposure to oxidative stress and DNA repair in skin cells. Scientific Reports, 15: 31214. DOI: https://www.doi.org/10.1038/s41598-025-15090-w

Hohlbaum K, Bert B, Dietze S, Palme R, and Fink H (2018). Impact of repeated anesthesia with ketamine and xylazine on the well-being of C57BL/6JRj mice. PLoS ONE, 13(9): e0203559. DOI: https://www.doi.org/10.1371/journal.pone.0203559

Hu Q, He Y, Wang F, Wu J, Ci Z, Chen L, Xu R, Yang M, and Lin J (2021). Microwave technology: A novel approach to the transformation of natural metabolites. Chinese Medicine, 16(1): 87. DOI: https://www.doi.org/10.1186/s13020-021-00500-8

Hu X, Shi C, and De Schutter G (2016). A review on microstructure characterization of cement-based materials subjected to chloride by AC impedance. Sustainable Construction Materials and Technologies (SCMT 2016), pp. 1-11. Available at: https://backoffice.biblio.ugent.be/download/8531798/8535829

Hu X, Shi C, Liu X, Zhang J, and de Schutter G (2019). A review on microstructural characterization of cement-based materials by AC impedance spectroscopy. Cement and Concrete Composites, 100: 1-14. DOI: https://www.doi.org/10.1016/j.cemconcomp.2019.03.018

Hu X, Shi C, Yuan Q, and de Schutter G (2020). AC impedance spectroscopy characteristics of chloride-exposed cement pastes. Construction and Building Materials, 233: 117267. DOI: https://www.doi.org/10.1016/j.conbuildmat.2019.117267

International commission on non-ionizing radiation protection (ICNIRP) (2020). ICNIRP guidelines for limiting exposure to electromagnetic fields (100 kHz to 300 GHz). Health Physics, 118(5): 483-524. DOI: https://www.doi.org/10.1097/HP.0000000000001210

Ikinci A, Randel J, and Odaci E (2019). Changes in pyramidal and granular neuron numbers in the rat hippocampus 7 days after exposure to a continuous 900-MHz electromagnetic field during early and mid-adolescence. Journal of Chemical Neuroanatomy, 101: 101681. DOI: https://www.doi.org/10.1016/j.jchemneu.2019.101681

Jagetia GC (2022). Genotoxic effects of electromagnetic field radiations from mobile phones. Environmental Research, 212: 113321. DOI: https://www.doi.org/10.1016/j.envres.2022.113321

Jamal MA, Ahmed AM, Tahir M, Ashraf M, Sattar A, Ghafoor A, Munir S, Ahmed I, Hussain M, and Riaz A (2019). Safety and efficacy of ketamine–xylazine along with atropine anesthesia in BALB/c mice. Brazilian Journal of Pharmaceutical Sciences, 55: e17231. DOI: https://www.doi.org/10.1590/s2175-97902019000317231

Javaeed A, Qamar S, Ali S, Mustafa MAT, Nusrat A, and Ghauri SK (2021). Histological stains in the past, present, and future. Cureus, 13(10): e18486. DOI: https://www.doi.org/10.7759/cureus.18486

Ji DH, Ni YF, Lin CY, and Yeh MY (2025). Transparent and stretchable conductive hydrogel sensors: Optimizing ion selection to enhance mechanical and sensing performance. ACS Applied Electronic Materials, 7(2): 874-883. DOI: https://www.doi.org/10.1021/acsaelm.4c02101

Katheriya T, Pandey S, and Upadhyay S (2025). New frontiers in ceramic composites: Tunable electromagnetic interference shielding by realizing negative permittivity in SnO_2/$LaNiO_3$ nanocomposites. Journal of Materials Chemistry C, 13(26): 13154-13166. DOI: https://www.doi.org/10.1039/D5TC01396H

Kim HS, Choi HD, Pack JK, Kim N, and Ahn YH (2021). Effects of radiofrequency electromagnetic field exposure on the placental barrier in pregnant mice. Bioelectromagnetics, 42(2): 191-199. DOI: https://www.doi.org/10.1002/bem.22322

Kumar N and Kuanr BK (2024). Lightweight and thin with high-frequency performance microwave absorbing heterostructure carbon derived from Ashoka-leaf ash. Research Square (Preprint). DOI: https://www.doi.org/10.21203/rs.3.rs-3913745/v1

Lahiri YK (2023). Non-ionizing radiations and their biochemical and biomedical impacts: A review. Journal of Radiation and Cancer Research, 14(1): 53-66. DOI: https://www.doi.org/10.4103/jrcr.jrcr_17_22

Lai H (2021). Genetic effects of non-ionizing electromagnetic fields. Electromagnetic Biology and Medicine, 40(2): 264-273. DOI: https://www.doi.org/10.1080/15368378.2021.1881866

Lai H and Levitt BB (2024). Cellular and molecular effects of non-ionizing electromagnetic fields. Reviews in Environmental Health, 39(3): 519-529. DOI: https://www.doi.org/10.1515/reveh-2023-0023

Leach VA, Yakymenko I, De Iuliis GN, and Chrousos GP (2025). A comprehensive mechanism of biological and health effects of anthropogenic extremely low frequency and wireless communication electromagnetic fields. Frontiers in Public Health, 13: 1585441. DOI: https://www.doi.org/10.3389/fpubh.2025.1585441

Lee Y, So JH, and Kim HJ (2024). A transparent hydrogel ionic conductor with high water retention and self-healing ability. Materials, 17(2): 288. DOI: https://www.doi.org/10.3390/ma17020288

Lesbayev A, Akalim D, Kalauov B, and Yerezhep D (2025). An investigation into Fe_3O_4 nanoparticle-based composites for enhanced electromagnetic radiation shielding. Journal of Composites Science, 9(5): 226. DOI: https://www.doi.org/10.3390/jcs9050226

Liang C, Gu Z, Zhang Y, Ma Z, Qiu H, and Gu J (2021). Structural design strategies of polymer matrix composites for electromagnetic interference shielding: A review. Nano-Micro Letters, 13(1): 181. DOI: https://www.doi.org/10.1007/s40820-021-00707-2

Liu N, Liu Y, Wang Y, Feng C, Piao M, and Liu M (2025). Oxidative cell death in the central nervous system: Mechanisms and therapeutic strategies. Frontiers in Cell and Developmental Biology, 13: 1562344. DOI: https://www.doi.org/10.3389/fcell.2025.1562344

Lodi MB, Bellizzi G, Paulis A, Grandi N, Palmeri R, Sekehravani EA, Crocco L, Fanti A, and Scapaticci R (2025). Electromagnetic characterization and biocompatibility assessment of magnetic materials for biomedical applications. 19th European Conference on Antennas and Propagation (EuCAP), Stockholm, Sweden, pp. 1-14. DOI: https://www.doi.org/10.23919/eucap63536.2025.10999465

Manolaras I, Del Bondio A, Griso O, Reutenauer L, Eisenmann A, Habermann BH, and Puccio H (2023). Mitochondrial dysfunction and calcium dysregulation in COQ8A-ataxia Purkinje neurons are rescued by CoQ10 treatment. Brain, 146(9): 3836-3850. DOI: https://www.doi.org/10.1093/brain/awad099

Meenu L, Aiswarya S, Menon KAU, and Menon SK (2025). Evaluating the impact of plant species on outdoor wireless communication by analyzing plant material characteristics. Proceedings of Photonics & Electromagnetics Research Symposium, Abu Dhabi, United Arab Emirates. DOI: https://www.doi.org/10.1109/piers-spring66516.2025.11276563

Mehmet Y, Kilitci A, Çelik E, Yegin K, Sirav B, and Varol S (2024). Effects of radiofrequency radiation exposure on rat brain and testicular tissue. International Journal of Radiation Research, 22(3): 529-536. DOI: https://www.doi.org/10.61186/ijrr.22.3.529

Mensah EE, Azis S, and Abbas Z (2022). Microwave absorption properties of recycled expanded polystyrene (EPS) and rice husk composites. Journal of Materials Science and Chemical Engineering, 10(3): 30-41. DOI: https://www.doi.org/10.4236/msce.2022.103003

Meyer F, Bitsch A, Jay H, Fragoulis A, Ghezzi P, Henschenmacher B, Kellner R, Kühne J, Ludwig T, Sachno D et al. (2024). Effects of radiofrequency electromagnetic field exposure on oxidative stress biomarkers: A systematic review. Environment International, 194: 108940. DOI: https://www.doi.org/10.1016/j.envint.2024.108940

Mizobuchi T, Yokozeki K, Watanabe K, Hiraishi M, and Ashizawa R (2026). Monitoring system for chloride content in concrete cover using electromagnetic wave and impedance methods. High-performance concrete, brick-masonry and environmental aspects. CRC Press, pp. 1-12. DOI: https://www.doi.org/10.1201/9781003759768-79

Muradyan AA, Aramyan AR, Alexanyan HA, Sargsyan NH, Mkrtchyan LS, and Harutyunyan VG (2025). Emergence of negative dielectric constant in dielectric materials. IEEE Transactions on Dielectrics and Electrical Insulation, 33(1): 1-10. DOI: https://www.doi.org/10.1109/TDEI.2025.3590690

Neres R, Romero C, and Marinho F (2008). Placenta pathology and pregnancy outcome in malaria-infected mic. PLoS ONE, 3(2): e1608. DOI: https://www.doi.org/10.1371/journal.pone.0001608

Orfali R, Alwatban AZ, Orfali RS, Lau L, Chea N, Alotaibi AM, and Nam Y (2024). Oxidative stress and ion channel dysfunction in neurodegenerative diseases. Frontiers in Physiology, 15: 1320086. DOI: https://www.doi.org/10.3389/fphys.2024.1320086

Pall ML (2016). Electromagnetic fields act via activation of voltage-gated calcium channels to produce beneficial or adverse effects. Current Chemical Biology, 10(1): 74-82. DOI: https://www.doi.org/10.2174/2212796810666160419160433

Panagopoulos DJ, Yakymenko I, De Iuliis GN, and Chrousos GP (2025) A comprehensive mechanism of biological and health effects of anthropogenic extremely low frequency and wireless communication electromagnetic fields. Frontiers in Public Health 13: 1585441. DOI: https://www.doi.org/10.3389/fpubh.2025.1585441

Płowaś-Korus I and Buchner R (2021). Hydration and aggregation phenomena in aqueous solutions of xylitol. Journal of Molecular Liquids, 340: 116838. DOI: https://www.doi.org/10.1016/j.molliq.2021.116838

Prashanth PVS, Jayamani E, and Soon KH (2024). Recent progress in bio-based polymer dielectric composites for electromagnetic interference shielding: A review. Renewable and Sustainable Energy Reviews, 209: 115026. DOI: https://www.doi.org/10.1016/j.rser.2024.115026

Reghunath R, Shadiya MA, Dileep P, Murali KP, and Paul J (2025a). Polymer-based composites for electromagnetic interference shielding: Recent advances and challenges. Polymers for Advanced Technologies, 36(9): 1-20. DOI: https://www.doi.org/10.1002/pat.70356

Reghunath R, Parveen KM, Murali KP, and Paul J (2025b). Magneto-dielectric fillers for electromagnetic interference shielding applications: A review. Engineering Research Express, 7(2): 022505. DOI: https://www.doi.org/10.1088/2631-8695/add8e4

Ren J, Mu Z, Sellami R, El-Bahy SM, Liang G, Guo J, El-Bahy ZM, Xie P, Guo Z, and Hou H (2025). Recent advances in microwave-absorbing materials: Design strategies and mechanisms. Advanced Composites and Hybrid Materials, 8(2): 1-25. DOI: https://www.doi.org/10.1007/s42114-025-01258-5

Rong Y, Guo H, Zhou X, Wu W, Zhu W, Wang H, Ma X, Jiang S, and Sun Q (2025). Recent progress in electromagnetic interference shielding materials: Mechanisms and applications. Advanced Functional Materials, 35(51): 2506746. DOI: https://www.doi.org/10.1002/adfm.202506746

Ruscica G, Peinetti F, Sora IN, and Savi P (2024). Electromagnetic shielding properties of cement-based composites: A review. Journal of Carbon Research, 10(1): 21. DOI: https://www.doi.org/10.3390/c10010021

Saliev T, Begimbetova D, Masoud AR, and Matkarimov B (2019). Biological effects of non-ionizing electromagnetic fields: Two sides of a coin. Progress in Biophysics and Molecular Biology, 141: 25-36. DOI: https://www.doi.org/10.1016/j.pbiomolbio.2018.07.009

Santo LE, Pereira CSGP, Costa ASG, Almeida A, Barreira JCM, Oliveira MBPP, and Vinha AF (2025). Bioactive differentiation of Opuntia fruits and by-products: A comparative analysis. Foods, 14(18): 3170. DOI: https://www.doi.org/10.3390/foods14183170

Schuermann D and Mevissen M (2021). Manmade electromagnetic fields and oxidative stress—biological effects and consequences for health. International Journal of Molecular Sciences, 22(7): 3772. DOI: https://www.doi.org/10.3390/ijms22073772

Shahin S, Singh VP, and Shukla RK (2013). 2.45 GHz microwave radiation induces oxidative stress and DNA damage in rat brain and pregnancy outcomes. Applied Biochemistry and Biotechnology, 169(6): 1727-1751. DOI: https://www.doi.org/10.1007/s12010-012-0079-9

Shi Y, Wu M, Ge S, Li J, Alshammari AS, Luo J, Amin MA, Qiu H, Jiang J, Asiri YM et al. (2025). Advanced electromagnetic shielding materials: Design strategies and mechanisms. Nano-Micro Letters, 17(1): 1-25. DOI: https://www.doi.org/10.1007/s40820-024-01494-8

Simón J, Villanueva-Maldonado J, Castillo-Soria FR, Cardenas-Juarez M, Briones E, Sandoval-Arechiga R, Soriano-Equigua L, and Alvarez-Flores JL (2019). Microwave absorption behavior of plant-based materials. International Journal of Chemical Engineering, 2019: 5872141. DOI: https://www.doi.org/10.1155/2019/5872141

Soria AC, Ruiz-Aceituno L, Ramos L, and Sanz ML (2021). Microwave-assisted extraction of bioactive compounds from plant materials. In: K. Ramawat and J. M. Mérillon (Editors), Protocols. Springer., Cham, pp. 1-18. DOI: https://www.doi.org/10.1007/978-3-319-03751-6_43-1

Tian H, Zhu H, Gao C, and Shi M (2022). System-level biological effects of extremely low-frequency electromagnetic fields: An in vivo experimental review. Frontiers in Neuroscience, 16: 124702. DOI: https://www.doi.org/10.3389/fnins.2023.1247021

Toader C and Covache-Busuioc R (2025). The redox revolution in brain medicine: Targeting oxidative stress with AI, multi-omics and mitochondrial therapies for the precision eradication of neurodegeneration. International Journal of Molecular Sciences, 26(15): 7498. DOI: https://www.doi.org/10.3390/ijms26157498

Tzaneva B and Kostov V (2023). Corrosion behaviour of heterogeneous antimony–copper layers in chloride media. Corrosion Engineering, Science and Technology, 58(8): 677-686. DOI: https://www.doi.org/10.1080/1478422X.2023.2247661

Verbeek J, Oftedal G, Feychting M, van Rongen E, Rosaria Scarfì M, Mann S, Wong R, and van Deventer E (2021). Prioritizing health outcomes when assessing the effects of exposure to radiofrequency electromagnetic fields: A survey among experts. Environment International, 146: 106300. DOI: https://www.doi.org/10.1016/j.envint.2020.106300

Wang X, Wei Z, Huang Z, Su T, Miao Y, and Gao F (2023). Dielectric properties and electromagnetic wave absorption performance of glass/ceramic composites. Journal of Materials Science: Materials in Electronics, 34(22): 2299-2312. DOI: https://www.doi.org/10.1007/s10854-023-11760-5

Zhang X, Qiao J, Jiang Y, Wang F, and Tian X (2021). Metal–organic framework-derived carbon materials for electromagnetic wave absorption. Nano-Micro Letters, 13(1): 135. DOI: https://www.doi.org/10.1007/s40820-021-00658-8

Zhang C, Wang D, Dong L, Li K, Zhang Y, Yang P, and Yi S (2022). Enhanced microwave absorption performance of α-Fe_2O_3-based composites: Mechanism and design. International Journal of Molecular Sciences, 23(16): 9362. DOI: https://www.doi.org/10.3390/ijms23169362

Zhang M, Zheng Q, Cao WQ, and Cao MS (2025). Dielectric tuning of graphene-based hybrid materials for high-performance electromagnetic wave absorption. Materials Horizons, 12(5): 1440-1451. DOI: https://www.doi.org/10.1039/D4MH01351D

Zheng W, Ye W, Yang P, Wang D, Xiong Y, Liu Z, Qi J, and Zhang Y (2022). Iron-based composites for efficient microwave absorption: Synthesis and electromagnetic properties. Molecules, 27(13): 4117. DOI: https://www.doi.org/10.3390/molecules27134117